STUDIES OF BEAM-BEAM INTERACTIONS IN RUN IIa AT THE TEVATRON

T. Sen, Y. Alexahin, B. Erdelyi and M. Xiao
FNAL, Batavia, IL 60510, USA

Abstract

We discuss the impact of the beam-beam interactions on Run IIa operation at the design parameters. We focus on the seventy long-range interactions which primarily determine the stable region in phase space and limit the lifetime. We discuss recent improvements in lifetime at injection and dynamic aperture calculations at collision.

1 INTRODUCTION

In Run IIa the Tevatron is operating with 36 proton and 36 anti-proton bunches. This is a six-fold increase in the number of bunches per beam compared to Run I. The beam-beam interactions may be characterized as weak-strong since the proton intensities are an order of magnitude higher than anti-proton intensities. Each anti-proton bunch experiences seventy two long-range interactions during injection and ramping while at collision there are seventy long-range interactions and two head-on interactions at the two experiments CDF and D0. The long-range interactions have a strong influence on the anti-protons at all stages of the operational cycle but especially during injection and acceleration. Here we will report on the effects at injection with present proton intensities and at collision with design proton intensities which are about 35-40% higher than present values.

2 INJECTION

The Tevatron is initially filled with three trains of twelve proton bunches. The bunches are spaced 21 rf buckets apart. They are injected onto the central orbit and subsequently moved to a helical orbit before anti-protons are injected. The anti-protons are injected four bunches at a time into the abort gaps between the proton bunches. After the leading four bunches in each train is injected, the anti-protons are cogged by 84 rf buckets to make room for the next four bunches in the abort gap. The leading eight bunches in each train are cogged again by 84 buckets to allow the injection of the last four bunches in each train. After each train is full, the two beams are accelerated to top energy, the optics is changed to reduce β^* at the two interaction points (IPs) in a sequence of steps to the collision value and a final cogging by 61 buckets is done to align the two beams longitudinally at the IPs. The beams are still transversely separated at this point so the beams are brought into collision by collapsing the separation bumps.

One of the key observations at injection is that the lifetime of the protons drops substantially when they are moved from the central orbit to the helical orbit. While there are several factors which have an impact on the lifetime (residual gas scattering is thought to be significant) the nonlinearities play a significant role. Figure 1 shows the dynamic aperture of particles when on the central orbit and on the anti-proton helix. Chromaticity and feed-down sextupoles and the field errors in the arc dipoles were included in this calculation. It is evident that the nonlinearities have a major impact as the average dynamic aperture drops by almost a factor of two when the particles are moved to the helical orbit from the central orbit (see Table 1).

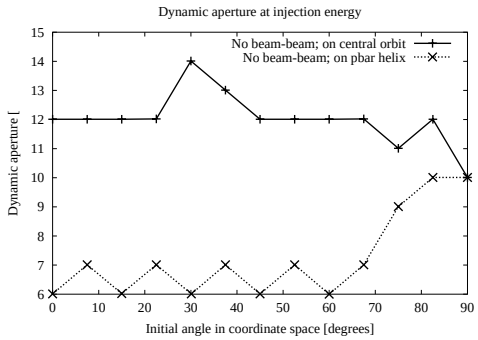

Figure 1: Dynamic aperture on the central orbit and on the anti-proton helix at injection energy without beam-beam interactions. Particles were tracked for 100,000 turns (2 secs in the Tevatron) with momentum deviations of $\Delta p/p = 4.3 \times 10^{-4}$. The horizontal axis is the initial angle of the particle in $x - y$ space while the vertical axis is the dynamic aperture in units of the rms beam size.

In addition to the machine nonlinearities, the anti-protons are also subject to the fields from the protons and their lifetimes are even lower than those of protons. The lifetime depends sensitively on the beam separations and recent efforts to increase the separations by changing the separator voltages have nearly doubled the anti-proton lifetime at injection. Figure 2 shows the separations with an earlier helix used up until April of this year and the new helix which improved performance. The separations shown are between anti-proton bunch 1 and the proton bunches at all seventy two long-range interactions soon after injection. The minimum separation with the old helix was about 4.7σ while with the new helix the minimum separation is about 6.8σ.

Figure 3 shows the small amplitude horizontal tune shift due to the beam-beam interaction with the old and new helices. The increased separation has reduced the small am-

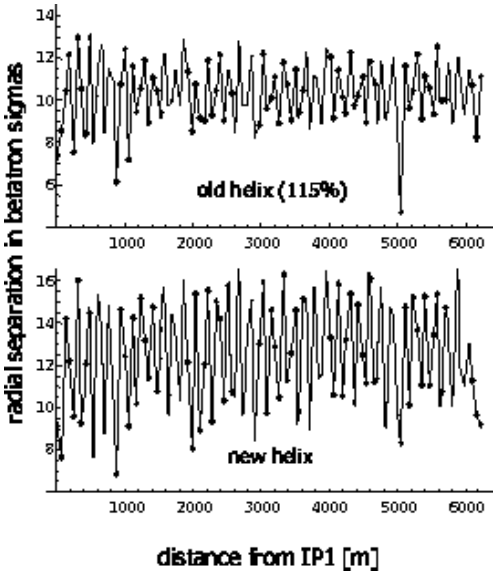

Figure 2: The old and new injection helix. Also shown as diamonds are the beam separation between anti-proton bunch 1 and proton bunches (in units of rms size) at all 72 parasitic locations.

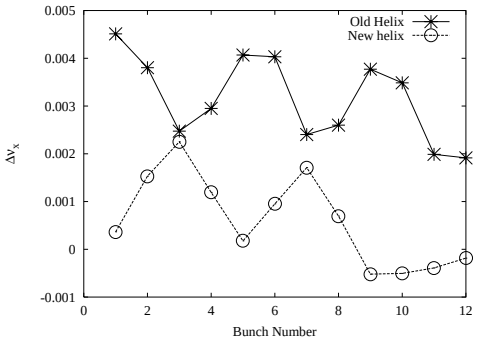

Figure 3: Change in the small amplitude horizontal tunes with the old and nex helix

plitude tune shifts for almost all the bunches significantly.

Table 1 shows the dynamic aperture of a single beam, first on the central orbit and on the anti-proton helix. It also shows the dynamic aperture of anti-proton bunch 1 at different cogging stages. The fact that the dynamic aperture is almost the same at all stages suggests that injecting the anti-protons at a different longitudinal position with respect to the protons may not improve the lifetime of the anti-protons at injection.

3 COLLISION

Once the beams are in collision, the average separations at the parasitic interactions are greater than 6σ except at the parasitics closest to the IPs on either side. Figure 4 shows the beam separations for anti-proton bunch 6 at the seventy parasitic locations and the zero separations at the IPs.

The dominant contributions to the tune spread are due to

	$(\langle DA \rangle, DA_{min})$
Without beam-beam	
On the central orbit	(12.0, 10.0)
On the pbar helix	(7.2, 6.0)
With beam-beam for pbar bunch 1	
No cogging	(5.3, 4.0)
After 1st cogging	(5.6, 5.0)
After 2nd cogging	(5.7, 5.0)

Table 1: Average and minimum dynamic aperture at injection - with and without the beam-beam interactions for anti-proton bunch 1

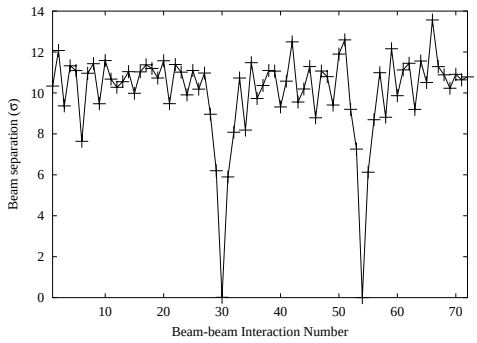

Figure 4: Separation between $\bar{p}$ bunch 6 and the opposing proton bunch at all 72 beam-beam interactions. The head-on collisions are at locations 30 (D0) and 54 (B0).

the head-on interactions with the next largest contributions from the nearest parasitics. Footprints of all bunches except for bunch 1 and 12 are clustered around that of bunch 6. The major differences in the tuneshifts between bunches 1 and 12 and all other bunches are due to the missing parasitic collision closest to the IP, upstream for bunch 1 and dowstream for bunch 12. Figure 5 shows the footprints due to the beam-beam interactions in Run IIa for bunches 1, 6 and 12.

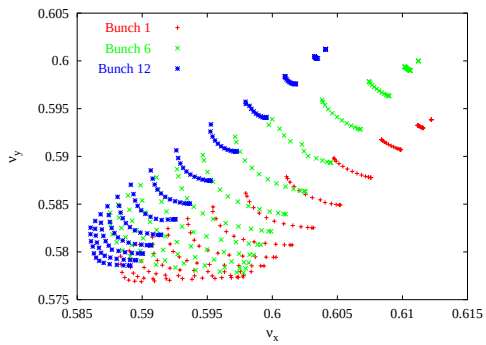

Figure 5: (color) Tune footprint for bunches 1, 6 and 12 in a train.

The parasitic interactions occur at locations of non-zero dispersion. Hence off energy anti-protons have different

separations from the opposing proton bunch and consequently experience a different tune shift. This leads to an amplitude dependent chromaticity or equivalently a chromaticity footprint [2]. Unlike the tune spread all the parasitics contribute in roughly equal measure to the chromaticity spread. Hence the synchro-betatron resonances driven by all the parasitics are important.

We have studied the relative importance of the beam-beam interactions by long term tracking. We find that the head-on interactions do not change the dynamic aperture by much. In 4D tracking (without energy deviations) the nearest parasitics reduce the dynamic aperture the most and the other parasitics have only a small influence. In 6D tracking (with energy oscillations) the other parasitics do have a significant impact on the dynamic aperture - as expected from their contributions to the chromaticity footprint. The results are summarized in Table 2.

Bunch 6: $\nu_x = 0.585, \nu_y = 0.575$ DA after 10^5 turns	$(\langle DA \rangle, DA_{min})$ [6D] $\Delta p/p = 3 \times 10^{-4}$
IR errors	(12.9, 11.0)
Head-on and IR errors	(12.5, 11.0)
Head-on, nearest PCs, IR errors	(8.9, 7.0)
Only the parasitics, IR errors	(7.7, 6.0)
All beam-beam, IR errors	(7.7, 6.0)

Table 2: The average and minimum 6D dynamic aperture with various configurations of beam-beam interactions.

Figure 6 compares the footprint including all beam-beam interactions with the footprint when the head-on interactions are excluded. The parasitics create a very small footprint yet we find that the dynamic aperture with only the parasitics is the same as that when the head-on interactions are included. Thus with beam-beam interactions there is no direct correlation between the size of the tune footprint and the dynamic aperture.

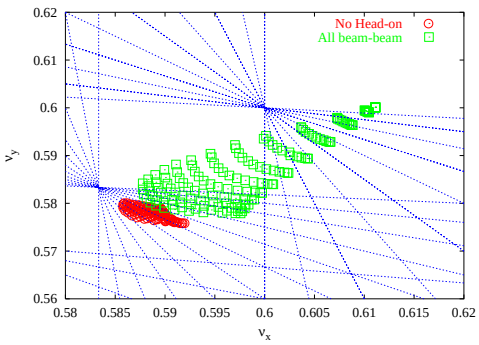

Figure 6: Comparison of the footprints including all beam-beam interactions with the footprint when the head-on interactions are excluded.

We have examined some of the mechanisms which lead to amplitude growth near the dynamic aperture. Diffusive growth would lead to a linear increase in time of the variance in action of an ensemble of particles. Instead the variance was found to stay nearly constant in time. Rather than diffusive growth we find that the region near the dynamic aperture is characterized by chaotic motion in narrow bands.

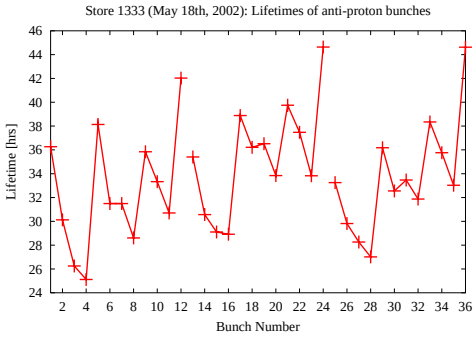

Figure 7: Measured lifetimes of all 36 anti-proton bunches during a recent luminosity run.

We have examined the differences in dynamic aperture between bunch 6 (in the center of a train) and bunches 1 and 12 at the two ends of the train. We find that these bunches have nearly the same dynamic aperture. Observations however show that the lifetime can vary greatly from one bunch to the next. Figure 7 shows the different lifetime of all 36 anti-proton bunches during a recent store. The largest lifetimes - around 46 hours - are close to the lifetimes expected simply from the loss of anti-protons during collisions. The lifetimes of these bunches (e.g bunch 12 in a train) do not seem to be strongly influenced by the parasitic interactions. Other bunches, e.g. bunch 4 in a train, have less than 30 hour lifetimes.

There are several possible reasons for these large variations. During injection there are natural variations in the anti-proton emittance and also in the proton emittance. Also at injection the physical acceptance is small and it is likely that bunches are scraped before accleration to top energy. Analysis of the luuminosity store in Figure 7 showed that the emittance of bunch 4 was larger than that of bunches 1 and 12 at the ends of the train.

4 REFERENCES

[1] T. Sen and M. Xiao,*Beam-beam interactions in Run IIa*, FNAL report to be published

[2] B. Erdelyi and T. Sen,*Analytic Studies of Long Range Beam-Beam Tune Shifts and Chromaticities*, this conference